

## A Theoretical Study of the Large Hg–Hg Spin–Spin Coupling Constants in $\text{Hg}_2^{2+}$ , $\text{Hg}_3^{2+}$ , and $\text{Hg}_2^{2+}$ –Crown Ether Complexes

Jochen Autschbach,<sup>\*,†</sup> Ciprian D. Igna, and Tom Ziegler<sup>‡</sup>

Contribution from the Department of Chemistry, University of Calgary,  
Calgary, Alberta, Canada T2N-1N4

Received September 26, 2002; E-mail: jochen.utschbach@chemie.uni-erlangen.de

**Abstract:** Nuclear spin–spin coupling constants  $^1J(\text{Hg}–\text{Hg})$  in the systems  $\text{Hg}_2^{2+}$  and  $\text{Hg}_3^{2+}$  represent the largest coupling constants so far observed in NMR experiments. We have performed a computational study on these ions, on  $\text{Hg}_2^{2+}$  complexes with 18-crown-6 and 15-crown-5, and on  $\text{Hg}_3^{2+}$  with solvent molecules and counterions. The results obtained with our recently developed program for the density functional computation of heavy nucleus spin–spin coupling constants are in good agreement with experiments. The data reveal that the bare ions  $\text{Hg}_2^{2+}$  and  $\text{Hg}_3^{2+}$  would afford much larger coupling constants than those experimentally observed, with an upper limit of approximately 0.9 MHz for  $\text{Hg}_2^{2+}$ . This limit is much larger than that previously estimated by Hückel theory. It is demonstrated that in solution or due to complexation the experimentally determined values are much smaller than the free ion's coupling constants. With the help of intuitive MO arguments, it is illustrated how the environment strongly reduces the coupling constants in  $\text{Hg}_2^{2+}$  and  $\text{Hg}_3^{2+}$ . The two-bond coupling constant  $^2J(\text{Hg}–\text{Hg})$  in  $\text{Hg}_3^{2+}$  is also examined.

### 1. Introduction

Scalar nuclear spin–spin coupling constants between mercury atoms represent the largest experimentally known coupling constants. A well-known example is the one-bond coupling  $^1J(\text{Hg}–\text{Hg})$  in  $[\text{Hg}–\text{Hg}–\text{Hg}]^{2+}$  of 139.6 kHz in ref 1 which was the first Hg–Hg coupling ever reported and the largest known coupling constant of that time (1984). Currently the Hg–Hg coupling of 284.1 kHz of a complex of  $[\text{Hg}–\text{Hg}]^{2+}$  with the crown ethers 18-crown-6 and 15-crown-5 reported in 2001 is the largest experimentally observed coupling constant.<sup>2</sup> [All values here and in the following refer to the  $^{199}\text{Hg}$  nucleus.] The “world records” for the coupling constants between different nuclei are currently held by  $[(\text{NC})_5\text{Pt}–\text{Tl}]$  (71.1 kHz) and the related complexes  $[(\text{NC})_5\text{Pt}–\text{Tl}(\text{CN})_n]^{n-}$  (for  $^{205}\text{Tl}$  and  $^{195}\text{Pt}$ ).<sup>3,4</sup>

A relativistic density functional approach to calculate spin–spin coupling constants involving heavy nuclei has emerged only recently.<sup>5,6</sup> Previously reported semiempirical or ab initio methodology is currently not applicable to the rather large heavy atom systems under consideration in this work and/or not able to achieve a comparable accuracy which is necessary

in order to make numerical predictions with sufficient confidence (such as four-component Hartree–Fock,<sup>7</sup> scaling of hyperfine integrals in semiempirical<sup>8</sup> or DFT calculations,<sup>9</sup> or relativistic extended Hückel theory<sup>10</sup>). It is of great benefit to theoretically study NMR parameters of systems with metal–metal bonds because the experimentally observed values are determined by a—sometimes very sensitive—interplay between features of the metal–metal bond, relativistic effects, the influence of the ligands, and the influence of the solvent. For instance, we have been able to explain very unintuitive features of the Tl–C coupling constants and the large Pt–Tl coupling of 57 kHz (experimental value) in  $[(\text{NC})_5\text{Pt}–\text{Tl}(\text{CN})]^-$  as the result of an interplay between solvent effects, relativity, and the multicenter character of the bonds along the C–Pt–Tl–C axis.<sup>11</sup> Another example is the case of Pt–Pt coupling constants. They can differ by a factor of 10 for chemically closely related dinuclear Pt complexes. We have recently explained this unintuitive fact by the interplay between relativistic effects on the Pt–Pt bond and the strength of the ligand's  $\sigma$ -interaction with the Pt centers.<sup>12</sup> We shall here extend previous studies of spin–spin coupling in compounds containing heavy nuclei to mercury–mercury couplings. We shall in particular show how relativistic effects<sup>13,14</sup> can serve as a “magnifying glass” for the study of subtle effects on metal–metal bonds.

<sup>†</sup> Present address: Lehrstuhl für Theoretische Chemie, Universität Erlangen, Egerlandstrasse 3, D-91058 Erlangen, Germany.

<sup>‡</sup> E-mail: ziegler@ucalgary.ca.

- (1) Gillespie, R. J.; Granger, P.; Morgan, K. R.; Schrobilgen, G. J. *Inorg. Chem.* **1984**, *23*, 887–891.
- (2) Malleier, R.; Kopacka, H.; Schuh, W.; Wurst, K.; Peringer, P. *Chem. Commun.* **2001**, 51–52.
- (3) Maliarik, M.; Berg, K.; Glaser, J.; Sandström, M.; Tóth, I. *Inorg. Chem.* **1998**, *37*, 2910–2919.
- (4) Berg, K. E.; Glaser, J.; Read, M. C.; Tóth, I. *J. Am. Chem. Soc.* **1995**, *117*, 7550–7751.
- (5) Autschbach, J.; Ziegler, T. *J. Chem. Phys.* **2000**, *113*, 936–947.
- (6) Autschbach, J.; Ziegler, T. *J. Am. Chem. Soc.* **2001**, *123*, 3341–3349.

- (7) Enevoldsen, T.; Visscher, L.; Saue, T.; Jensen, H. J. A.; Oddershede, J. *J. Chem. Phys.* **2000**, *112*, 3493–3498.
- (8) Lobayan, R. M.; Aucar, G. A. *J. Mol. Struct.* **1998**, *452*, 1–11.
- (9) Khandogin, J.; Ziegler, T. *J. Phys. Chem. A* **2000**, *104*, 113–120.
- (10) Pyykkö, P.; Wiesenfeld, L. *Mol. Phys.* **1981**, *43*, 557–580.
- (11) Autschbach, J.; Ziegler, T. *J. Am. Chem. Soc.* **2001**, *123*, 5320–5324.
- (12) Autschbach, J.; Igna, C. D.; Ziegler, T. *J. Am. Chem. Soc.* **2003**, *125*, 1028–1032.
- (13) Pyykkö, P. *Chem. Rev.* **1988**, *88*, 563–594.

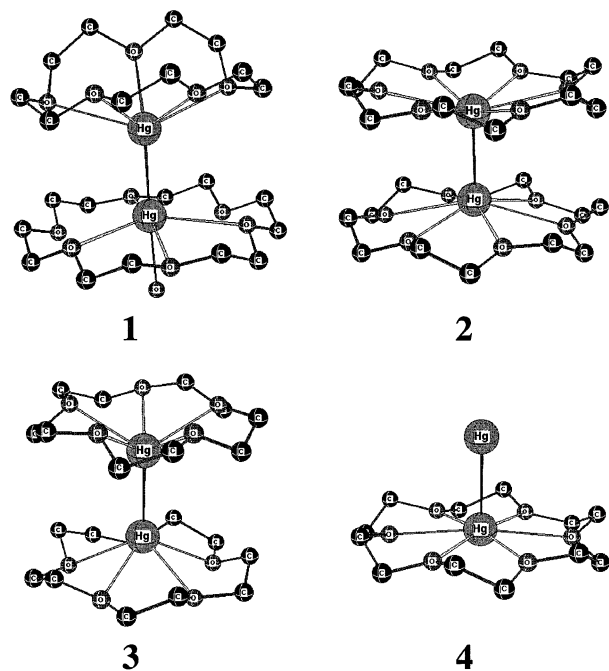


**Figure 1.**  $\text{Hg}_2^{2+}$ -crown ether complexes studied in this work.  $\text{Hg}_2^{2+}$ (15-crown-5)(18-crown-6) $\cdot\text{H}_2\text{O}$  **1** (crystal structure),  $\text{Hg}_2^{2+}$ (18-crown-6) $_2$  **2**,  $\text{Hg}_2^{2+}$ (15-crown-5) $_2$  **3**,  $\text{Hg}_2^{2+}$ (18-crown-6) **4**. Hydrogens are not displayed for clarity.

Because of the difficulties with a theoretical description of heavy atoms in general and their very sensitive NMR parameters in particular, no first-principles theoretical study of the largest known spin–spin coupling constants has so far been carried out. We will show that these quantities for the  $\text{Hg}_2^{2+}$  and  $\text{Hg}_3^{2+}$  ions can be reproduced by computations that take environmental effects into considerations. It is further our aim to report that the mechanisms that are responsible for the large differences in the metal–metal coupling constants for different complexes, and compared to computations on the free ions, can be rationalized with the help of simple MO models. On this basis, we suggest possible candidates to afford a Hg–Hg spin–spin coupling constant that could exceed the 284.1 kHz of ref 2 with a large margin.

Some of the systems that are studied here are depicted in Figures 1 and 2. In addition to the ions  $\text{Hg}_2^{2+}$  and  $\text{Hg}_3^{2+}$  in the gas phase, we have studied  $\text{Hg}_3^{2+}$  with varying numbers of solvent molecules ( $\text{SO}_2$ , **7–12** and others) and with counterions ( $\text{AsF}_6^-$ , **5, 6**), as well as  $\text{Hg}_2^{2+}$ -crown ether complexes with 15-crown-5 and 18-crown-6 (**1–4**). In section 2 we outline the details regarding the computations. In section 3 the results are interpreted and compared to experimental data. The findings are summarized in section 4.

## 2. Computational Details

The computations have been carried out with the Amsterdam density functional (ADF) program package.<sup>15–17</sup> It incorporates our recently

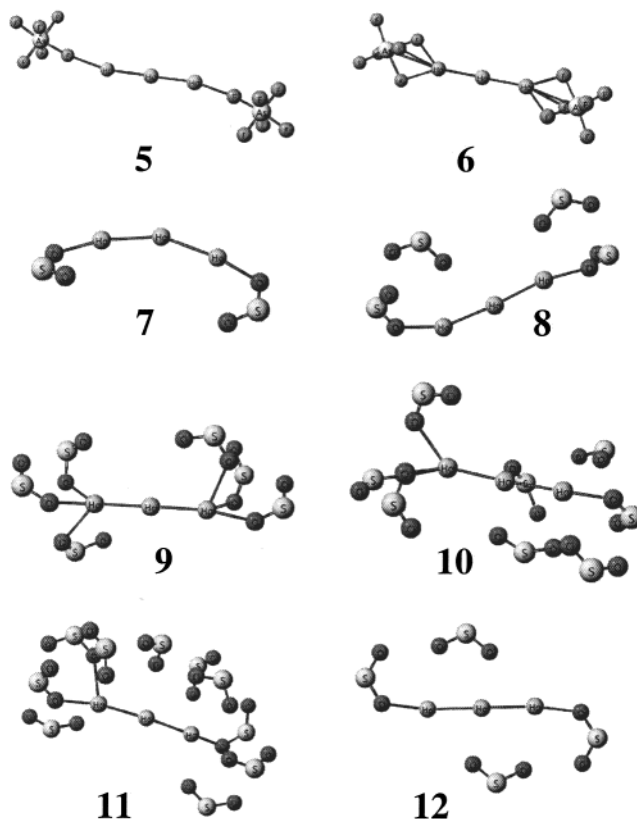


**Figure 2.**  $\text{Hg}_3^{2+}$  complexes with solvent molecules or counterions.  $\text{Hg}_3^{2+}$ ( $\text{AsF}_6^-$ ) $_2$  **5** and **6**,  $\text{Hg}_3^{2+}$  with various numbers of solvent molecules ( $\text{SO}_2$ ) **7–12**.

developed code for the two-component relativistic computation of nuclear spin–spin coupling constants,<sup>5,18</sup> based on the zeroth-order regular approximation (ZORA) Hamiltonian.<sup>19,20</sup> The computational settings that were applied here as well as details on the basis sets are described in refs 6 and 5 and are briefly sketched here for convenience. All computations employed the Vosko–Wilk–Nusair<sup>21</sup> local density functional (LDA) for the ground-state calculations and geometry optimizations. In addition, some systems have been calculated using the BP<sup>22–24</sup> gradient-corrected (GGA) density functional in order to demonstrate that the results are not very sensitive to the particular choice of the approximate density functional for the ground-state computation. Triple- $\zeta$  Slater-type basis sets with one polarization function for the valence shell have been applied in the computations. We have confirmed by a number of test calculations on the samples of this work, and previously published data on methylmercury halides, that the results would not be significantly improved by adding more polarization functions to the basis set. The geometries have been optimized using frozen core basis sets (1s frozen for C, N, O; 1s–2p frozen for S, 1s–4f frozen for Hg), whereas the computations of the spin–spin coupling constants have employed all electron basis sets that were augmented with 1s functions with exponents up to  $\sim 10^4$  for Hg in order to obtain a reasonably accurate description of the Fermi-contact term. We refer the reader to refs 5 and 18 for details. Unless explicitly stated otherwise, the computations of spin–spin coupling constants have been based on ZORA-optimized geometries.

(14) Schwarz, W. H. E. *Fundamentals of Relativistic Effects in Chemistry*. In *The Concept of the Chemical Bond*, Vol. 2; Masic, Z. B., Ed.; Springer: Berlin, 1990.

(15) Fonseca Guerra, C.; Visser, O.; Snijders, J. G.; te Velde, G.; Baerends, E. J. Parallelisation of the Amsterdam Density Functional program Program. In *Methods and Techniques for Computational Chemistry*; STEF: Cagliari, 1995.

(16) te Velde, G.; Bickelhaupt, F. M.; Baerends, E. J.; van Gisbergen, S. J. A.; Fonseca Guerra, C.; Snijders, J. G.; Ziegler, T. *J. Comput. Chem.* **2001**, *22*, 931–967.

(17) “Amsterdam Density Functional program”, Theoretical Chemistry, Vrije Universiteit, Amsterdam, URL: <http://www.scm.com>.

(18) Autschbach, J.; Ziegler, T. *J. Chem. Phys.* **2000**, *113*, 9410–9418.

(19) van Lenthe, E.; Baerends, E. J.; Snijders, J. G. *J. Chem. Phys.* **1993**, *99*, 4597–4610.

(20) Dyall, K.; van Lenthe, E. *J. Chem. Phys.* **1999**, *111*, 1366–1372.

(21) Vosko, S. H.; Wilk, L.; Nusair, M. *Can. J. Phys.* **1980**, *58*, 1200–1211.

(22) Becke, A. D. *Phys. Rev. A* **1988**, *38*, 3098–3100.

(23) Perdew, J. P. *Phys. Rev. B* **1986**, *33*, 8822–8824.

(24) Perdew, J. P. *Phys. Rev. B* **1986**, *34*, 7406.

**Table 1.**  $^{199}\text{Hg}$ – $^{199}\text{Hg}$  Spin–Spin Coupling Constants in  $\text{Hg}_2^{2+}$  and  $\text{Hg}_3^{2+}$  (in kHz)

|                     | $\text{Hg}_2^{2+}$    | $\text{Hg}_3^{2+}$                         |
|---------------------|-----------------------|--|
| ZORA LDA scalar     | 941.5 <sup>a</sup>    | 242.9 <sup>b,c</sup> /464.1 <sup>b,d</sup> |
| ZORA LDA SO         | 824.8 <sup>a</sup>    | 229.5 <sup>b,c</sup> /397.8 <sup>b,d</sup> |
| ZORA GGA scalar     | 935.8 <sup>a</sup>    | 241.8 <sup>b,c</sup> /460.4 <sup>b,d</sup> |
| ZORA GGA SO         | 819.8 <sup>a</sup>    | 241.0 <sup>b,c</sup> /452.6 <sup>b,d</sup> |
| Hückel <sup>e</sup> |                       | 80.00 <sup>e</sup>                         |
| REX <sup>f</sup>    | 274.5                 | 101.6 <sup>c</sup>                         |
| experiment          | 284.1(9) <sup>g</sup> | 139.7(3) <sup>c,h,i</sup>                  |

<sup>a</sup> This work. Scalar ZORA including the FC, OP, and OD term. Spin–orbit (SO) value additionally includes the SD term and spin–orbit cross terms  $R(\text{Hg}–\text{Hg}) = 2.638 \text{ \AA}$ . <sup>b</sup> This work. See also footnote a.  $R(\text{Hg}–\text{Hg}) = 2.665 \text{ \AA}$ . <sup>c</sup> One-bond coupling  $^1J(\text{Hg}–\text{Hg})$ . <sup>d</sup> Two-bond coupling  $^2J(\text{Hg}–\text{Hg})$ . <sup>e</sup> Estimate based on Hückel MOs and relativistically corrected hyperfine integrals for Hg 6s, ref 1. An alternative value of 142.4 kHz is also quoted in this reference, but the origin is unclear. <sup>f</sup> Relativistic EXtended Hückel theory (REX) with 6s + 6p basis, quoted in ref 28. <sup>g</sup> Crown ether complex **1** with one MeOH coordinating to Hg through the 18-crown-6 ring, in MeOH, ref 2. <sup>h</sup>  $\text{Hg}_3(\text{AsF}_6)_2$  in liquid  $\text{SO}_2$ , ref 1. <sup>i</sup>  $^2J(\text{Hg}–\text{Hg})$  not yet measured.

The spin–spin coupling constant within the relativistic ZORA formalism consists of four terms that we denote by Fermi-contact (FC), spin-dipole (SD), and the paramagnetic and diamagnetic orbital terms (OP and OD). We have chosen the well-known nonrelativistic nomenclature<sup>25</sup> for the four terms because, first, they yield the respective FC, SD, OP, and OD terms of Ramsey’s nonrelativistic theory in the nonrelativistic limit (speed of light  $c \rightarrow \infty$ ) and, second, they can be interpreted in a similar way.<sup>5,26</sup> Corrections to the spin–spin coupling constants arising from the electronic spin–orbit coupling have been evaluated as well for  $\text{Hg}_2^{2+}$  and  $\text{Hg}_3^{2+}$  and for two linear  $\text{Hg}_2^{2+}$  complexes. Because of their expense and a rather small effect in terms of their relative magnitude as compared to the scalar relativistic results, these corrections have been neglected for the larger systems. For the same reason, the expensive but often negligible SD term has been neglected in the scalar relativistic ZORA computations (it is, however, included in the spin–orbit calculations in which it hardly adds to the computational expense). All the calculated coupling constants are “classic”<sup>27,28</sup> in the sense that they are almost completely determined by the FC term. Therefore, the qualitative analysis has been restricted to this contribution. For instance, for the coupling constants listed in Table 3 below the OP contribution does not exceed 0.1 kHz in magnitude and is typically negative. The same is true for the bare ions (Table 1). For counter examples in which the OP term dominates the coupling constant, see, for example, ref 29. Examples for which the spin–orbit corrections yield the dominant contribution to the spin–spin coupling constants are also known.<sup>6,18</sup>

### 3. Results and Discussion

**The Bare Ions.** The results for our calculations on the bare ions  $\text{Hg}_2^{2+}$  and  $\text{Hg}_3^{2+}$  are listed in Table 1, together with experimental values for the  $\text{Hg}_2^{2+}$ –18-crown-6–15-crown-5 complex in MeOH and for  $\text{Hg}_3(\text{AsF}_6)_2$  in liquid  $\text{SO}_2$ . Other available theoretical data for  $\text{Hg}_3^{2+}$  were obtained in 1993 with the relativistic extended Hückel (REX) model,<sup>30</sup> or in 1984 with a simple Hückel model employing a “relativistic value” for the Hg 6s density at the nucleus and an experimental estimate for the  $\sigma_g - \sigma_g^*$  orbital energy difference.<sup>1</sup> It can be seen from

Table 1 that our density functional calculations on  $\text{Hg}_3^{2+}$  are in worse agreement with the experimental data than the simple LCAO estimate by Gillespie et al.<sup>1</sup> or the REX values.<sup>28</sup> The results for  $\text{Hg}_2^{2+}$  based on computations for the bare ion are even more unsatisfactory since they overestimate the experimental value for the crown ether complex by more than a factor of 3. Again, the Hückel calculations for the bare  $\text{Hg}_2^{2+}$  are much closer to experiment. Fortunately, we can now (and must) go beyond computing the bare ions. We will show in the following that the ZORA DFT computations are likely to predict the correct magnitude of the coupling constants for the bare ions.

Regarding the influence of the approximations to the density functional in the ground-state computations, Table 1 lists results obtained with the local density approximation (LDA, in form of the VWN functional) and with a generalized gradient approximations (GGA, in form of the BP functional). At the nonrelativistic level for light atomic molecules, it is known that the quality of the functional has severe consequences for the accuracy of the final results.<sup>31–34</sup> However, we<sup>5</sup> have previously found that this is much less the case for the NMR properties of a heavy nucleus (except for “problematic cases”). It is known that for heavy atoms such as Hg simple functionals derived from the electron gas approximation already perform rather satisfactory, which is in contrast to light elements. The choice of a particular flavor of a (nonhybrid) GGA has been found to affect the results only marginally in the case of  $^{199}\text{Hg}$  chemical shifts.<sup>26,35</sup> For spin–spin coupling constants the results were found to be comparatively insensitive to the approximations (LDA versus GGA) to the density functional in case the coupling constant is dominated by the FC term,<sup>5,18</sup> as is the case for the systems studied in the present work. This is also illustrated by the data of Table 1. Due to the sensitivity of spin–spin coupling constants in general, the results are of course somewhat affected, but to an extent that is insignificant for the following discussion.

The results are also dependent on whether spin–orbit coupling is included in the computations or not.  $^1J(\text{Hg}–\text{Hg})$  in  $\text{Hg}_2^{2+}$  is affected by as much as 0.1 MHz (see footnote a in Table 1), a 14% correction that is certainly not negligible. On the other hand, previous experience and also additional computations on  $\text{Hg}_2\text{Cl}_2$  and  $\text{Hg}_2(\text{CN})_2$  indicate that the spin–orbit corrections contribute a certain fraction of the FC term to the final result rather than an absolute amount of 0.1 MHz in the case of  $\text{Hg}_2^{2+}$  and its complexes (Table 2). From the data in Table 2 it can be seen that the spin–orbit corrections only amount to 3% at most for these systems. The differences in the results for the LDA and the GGA functional, respectively, are 6% and smaller, in line with the argument of the preceding paragraph. For that reason we regard it as sufficient to treat the larger systems in the following sections at the scalar relativistic LDA level. (For complexes **2** and **3**, footnotes e and h of Table 3 list also scalar relativistic GGA values for comparison, with differences of only 3% and 5%, respectively, to the LDA results.) Thus for the systems studied in this work the conclusions, trends, and semiquantitative agreement with the experi-

(25) Pyykkö, P. *Theor. Chem. Acc.* **2000**, *103*, 214–216.

(26) Wolff, S. K.; Ziegler, T.; van Lenthe, E.; Baerends, E. J. *J. Chem. Phys.* **1999**, *110*, 7689–7698.

(27) Kowalewski, J. *Annu. Rep. NMR Spectrosc.* **1982**, *12*, 81–176.

(28) Contreras, R. H.; Facelli, J. C. *Annu. Rep. NMR Spectrosc.* **1993**, *27*, 255–356.

(29) Bryce, D. L.; Wasylishen, R. E.; Autschbach, J.; Ziegler, T. *J. Am. Chem. Soc.* **2002**, *124*, 4894–4900.

(30) Pyykkö, P.; Snijders, J. G.; Baerends, E. J. *Chem. Phys. Lett.* **1981**, *83*, 432–437.

(31) Helgaker, T.; Jaszunski, M.; Ruud, K. *Chem. Rev.* **1999**, *99*, 293–352.

(32) Patchkovskii, S.; Autschbach, J.; Ziegler, T. *J. Chem. Phys.* **2001**, *115*, 26–42.

(33) Helgaker, T.; Watson, M.; Handy, N. C. *J. Chem. Phys.* **2000**, *113*, 9402–9409.

(34) Sychrovský, V.; Gräfenstein, J.; Cremer, D. *J. Chem. Phys.* **2000**, *113*, 3530–3547.

(35) Jokisaari, J.; Järvinen, S.; Autschbach, J.; Ziegler, T. *J. Phys. Chem. A* **2002**, *106*, 9313–9318.



**Table 2.**  $^{199}\text{Hg}$ – $^{199}\text{Hg}$  Spin–Spin Coupling Constants in  $\text{Hg}_2\text{Cl}_2$  and  $\text{Hg}_2(\text{CN})_2$  (in kHz), from DFT Computations

|                 | $\text{Hg}_2\text{Cl}_2^a$ | $\text{Hg}_2(\text{CN})_2^b$ |
|-----------------|----------------------------|------------------------------|
| ZORA LDA scalar | 65.91                      | 46.73                        |
| ZORA LDA SO     | 64.89                      | 45.35                        |
| ZORA GGA scalar | 68.44                      | 48.52                        |
| ZORA GGA SO     | 66.67                      | 47.95                        |

<sup>a</sup> This work. Scalar ZORA including the FC, OP, and OD terms. Spin–orbit (SO) values additionally including the SD term and spin–orbit cross terms. Linear geometry,  $R(\text{Hg}–\text{Hg}) = 2.557 \text{ \AA}$ ,  $R(\text{Hg}–\text{Cl}) = 2.300 \text{ \AA}$ .<sup>b</sup> This work. See also footnote a. Linear geometry,  $R(\text{Hg}–\text{Hg}) = 2.572 \text{ \AA}$ ,  $R(\text{Hg}–\text{C}) = 2.046 \text{ \AA}$ ,  $R(\text{C}–\text{N}) = 1.161 \text{ \AA}$ .

**Table 3.**  $^{199}\text{Hg}$ – $^{199}\text{Hg}$  Spin–Spin Coupling Constants in  $\text{Hg}_2^{2+}$  Crown Ether Complexes (in kHz)<sup>a</sup>

| structure                      | $^1J(\text{Hg}–\text{Hg})$ | structure                   | $^1J(\text{Hg}–\text{Hg})$ |
|--------------------------------|----------------------------|-----------------------------|----------------------------|
| <b>1</b> expt.                 | 284.1(9) <sup>b</sup>      | <b>2</b> ·2H <sub>2</sub> O | 322.0 <sup>g</sup>         |
| <b>1</b>                       | 278.4 <sup>c</sup>         | <b>3</b>                    | 236.4 <sup>h</sup>         |
| <b>1</b> (no H <sub>2</sub> O) | 359.7 <sup>d</sup>         | <b>4</b>                    | 164.1 <sup>i</sup>         |
| <b>2</b>                       | 594.9 <sup>e</sup>         | <b>4</b> ·2H <sub>2</sub> O | 199.5 <sup>j</sup>         |
| <b>2</b> ·H <sub>2</sub> O     | 444.8 <sup>f</sup>         | <b>4</b> ·4H <sub>2</sub> O | 368.1 <sup>k</sup>         |

<sup>a</sup> Scalar ZORA LDA values for computational data, including the FC, OP, and OD terms. <sup>b</sup> Experimental value, see footnote g in Table 1. <sup>c</sup> Computation based on crystal structure from ref 2.  $R(\text{Hg}–\text{Hg}) = 2.520 \text{ \AA}$ . <sup>d</sup> Same structure as in c but without oxygen coordinating Hg through 18-crown-6 ring. <sup>e</sup> Optimized structure,  $D_6$  symmetry.  $R(\text{Hg}–\text{Hg}) = 2.585 \text{ \AA}$ . The scalar ZORA GGA result is 610.2 kHz. <sup>f</sup> Optimized structure of e with one H<sub>2</sub>O added. Oxygen coordinating Hg through one of the 18-crown-6 rings. Hg–O distance of 2.220  $\text{ \AA}$  of crystal structure c used without reoptimizing the whole system. <sup>g</sup> Same as f but with a coordinating oxygen in each ring. <sup>h</sup> Optimized structure,  $D_5$  symmetry.  $R(\text{Hg}–\text{Hg}) = 2.580 \text{ \AA}$ . The scalar ZORA GGA result is 249.0 kHz. <sup>i</sup> Optimized structure,  $C_6$  symmetry.  $R(\text{Hg}–\text{Hg}) = 2.731 \text{ \AA}$ .  $^1J(\text{Hg}–\text{Hg}) = 191.7 \text{ kHz}$  if structure of e is used and one of the 18-crown-6 rings is removed (no reoptimization). <sup>j</sup> Optimized structure of i with two H<sub>2</sub>O added in axial positions (one on each side of the  $\text{Hg}_2^{2+}$  fragment). Experimental Hg–O distance used as in f without reoptimizing the whole system. <sup>k</sup> Same as j but with three H<sub>2</sub>O added at the free Hg to result in tetrahedral coordination. Experimental Hg–O distance of used without reoptimizing the whole system.

mental data would not be significantly affected by the computationally expensive inclusion of spin–orbit coupling or the choice of a different LDA or GGA functional of the same quality. “Significant” refers here to the accuracy of the computations when compared to experimental data.

**[Hg–Hg]<sup>2+</sup> Crown Ether Complexes.** From our previous work,<sup>6,11,12</sup> it has become clear that ligands and solvent effects must be explicitly considered when attempting to understand and reproduce experimental NMR data for heavy metals by theoretical methods. This becomes strikingly obvious when computing  $^1J(\text{Hg}–\text{Hg})$  for the 18-crown-6–15-crown-5 complex of  $\text{Hg}_2^{2+}$  (**1**), employing the experimentally determined crystal structure of ref 2 (see Table 3). The scalar ZORA LDA result of 278.4 kHz based on this structure is in almost perfect agreement with the experimental value of 284.1 kHz for the Hg–Hg coupling. With the discussion of the previous section in mind, we assume that the spin–orbit corrections constitute a comparable fraction of the total value as in the free ion (approximately 15%) or less. This would still lead to very good agreement with the experimental value, taking into consideration the sensitivity of the coupling constant and the fact that small geometry changes due to molecular vibrations at finite temperature, or solvent effects, can easily lead to corrections of this magnitude. From the crystal structure of **1**, it can be seen that the 18-crown-6 ring is large enough in diameter in order to allow for an oxygen atom closely coordinating to one of the mercuries. In the crystal structure, this oxygen belongs to a water molecule.

For the computations we have thus decided to saturate the oxygen with hydrogen. In solution, the oxygen atom of a MeOH can also coordinate to the Hg through the large 18-crown-6 ring (note that the crystal structure exhibits two distinct subunits of the form **1**, one with a coordinating water molecule and one in which the coordinating oxygen belongs to a DMSO molecule; the experimental  $^1J(\text{Hg}–\text{Hg})$  for **1** has been attributed to the corresponding complex with MeOH by the authors of ref 2). To investigate why  $^1J(\text{Hg}–\text{Hg})$  is so strongly reduced for **1** compared to the free ion, we have carried out computations for this and other crown ether complexes, **2**, **3**, and **4**, including or excluding some water molecules. The results are also listed in Table 3. The data reveal that a strong reduction of  $^1J(\text{Hg}–\text{Hg})$  with respect to the free  $\text{Hg}_2^{2+}$  ion occurs in all cases, but in particular if the  $[\text{Hg}–\text{Hg}]^{2+}$  fragment is coordinated in a more axial position (i.e., along the Hg–Hg axis). From the structures **1**, **2** and **3**, it can be seen that the smaller crown ether, 15-crown-5, adopts a more axial coordination to Hg, i.e., trans to the other Hg, whereas 18-crown-6 almost completely surrounds each Hg and therefore leads to a more equatorial coordination. The Hg–Hg–O angles are 103° and 118° for **2** and **3**, respectively. For **1**, the angles with respect to 18-crown-6 range between 90° and 109°, and with respect to 15-crown-5 between 107° and 153°. Accordingly,  $^1J(\text{Hg}–\text{Hg})$  is much larger in **2** as compared to **3** or **1**, though still substantially smaller than for the free ion. When coordinating oxygen atoms (H<sub>2</sub>O) are added to **2** in the axial position, the coupling constant drops significantly. Still, on the basis of the computational data, we estimate the coupling constant for **2** in MeOH to be larger than the currently largest  $^1J(\text{Hg}–\text{Hg})$  of complex **1** even if such a coordination of Hg through the 18-crown-6 rings occurs. Because 15-crown-5 coordinates in a more axial position as compared to 18-crown-6, the computed Hg–Hg coupling constant of **3** is “only” of the same size as for **1** (see Table 3). For the latter,  $^1J(\text{Hg}–\text{Hg})$  can be expected to increase if coordination of the Hg through the 18-crown-6 ring could be prevented (see Table 3).

A surprising case is **4** because  $^1J(\text{Hg}–\text{Hg})$  is much smaller than for any of the other systems, even though the Hg–Hg–O angles are only 103° and the lesser coordination of the  $\text{Hg}_2^{2+}$  fragment could potentially be expected to lead to an increased Hg–Hg coupling constant. If this complex is coordinated at the free Hg by a number of water molecules in the computations,  $^1J(\text{Hg}–\text{Hg})$  becomes larger again, thereby approaching or possibly even exceeding the one for **2** with 2H<sub>2</sub>O. This is in apparent contradiction to the findings of the previous paragraph for the complexes with two crown ethers.

For a qualitative discussion of  $^1J(\text{Hg}–\text{Hg})$ , it is useful to employ the Hückel molecular orbital model. There are two distinct effects that need to be described in order to explain the features of the coupling constant: *coordination* by ligands or solvent molecules and *polarization* of the electron density of  $\text{Hg}_2^{2+}$  by an unsymmetric arrangement of the environment. We first note that in orbital-based approaches the dominant Fermi-contact contribution to the coupling constant between nucleus A and B can, for a homonuclear system with only one atomic s orbital (Hg 6s here) per atom considered, be written as

$$J^{\text{FC}}(\text{A}–\text{B}) = \text{const.} \cdot \sum_i^{\text{occ}} \sum_a^{\text{unocc}} \frac{C_i(\text{A})C_a(\text{A}) \cdot C_i(\text{B})C_a(\text{B})}{\epsilon_a - \epsilon_i} \quad (1)$$

Here, the  $C(X)$ 's are the coefficient for the 6s AO of atom X in the occupied (i) or unoccupied (a) MOs, with the  $\epsilon$ 's being the orbital energies. For the system  $\text{Hg}_2^{2+}$ , an orthonormal set of two orbitals  $\varphi$  (one occ, one unocc) built from the two 6s AOs ( $s_A$  and  $s_B$ ) is given as

$$\varphi_1 = \sin(x)s_A + \cos(x)s_B \quad (2a)$$

$$\varphi_2 = \cos(x)s_A - \sin(x)s_B \quad (2b)$$

with  $x$  ranging from 0 to  $\pi/2$ .  $\varphi_1$  shall be the occupied MO. The Hückel MOs of  $\text{Hg}_2^{2+}$  are given by letting  $x = \pi/4$ ,  $\sin(\pi/4) = \cos(\pi/4) = 1/\sqrt{2}$ , leading to symmetry-adapted  $\sigma$  and  $\sigma^*$  orbitals. If we assume to a first approximation that a polarization of the molecule due to the environment will not change the orbital energy difference ( $\epsilon_2 - \epsilon_1$ ) very much, the coupling constant in this basis of MOs is from eq 1 seen to be proportional to  $\sin(x)\cos(x)$ , i.e., proportional to  $\sin(2x)$ . Within the allowed range for  $x$ , the maximum is obtained for the unperturbed symmetric Hückel orbitals,  $x = \pi/4$ . An increasing orbital energy gap due to a more unsymmetric environment, which needs to be considered next, further leads to a decreased coupling constant as can be seen from eq 1. Consequently a polarization of the  $\text{Hg}_2^{2+}$  fragment can be expected to yield a smaller coupling constant, which appears to be the case for **4**. Note that we obtain 6s populations of 0.7 and 1.6 for the two Hg atoms in **4**, as compared to 0.9/1.1 for the mixed crown ether **1**, 0.8/1.2 for **4** with two water molecules added, and 1.0/1.0 for **2**. Adding additional coordinating solvent molecules on the “bare” side of the complex reduces the imbalance between the two Hg atoms and increases the coupling constant again.

The effect of a coordinating ligand in axial position has been previously analyzed by us<sup>12</sup> for the case of Pt–Pt bonds and can be qualitatively transferred to the case of  $\text{Hg}_2^{2+}$  without modifications. We summarize the results here for convenience. On the basis of a simple MO model, the fact that a ligand binds to the metal–metal fragment means to a first approximation that the antibonding  $\sigma^*$  mixes with the occupied ligand orbitals. This reduces the s character of the Hg–Hg bond and consequently leads also to a reduction of the spin–spin coupling constant that is more pronounced the stronger the  $\sigma$ -interaction between the metal and the ligand is. The analysis of the computational data in the case of the Pt–Pt systems has shown that this effect is particularly strong if the coordinating ligand is opposite to the other metal, a feature which is also emerging from the data for the mercury complexes studied in this work. In a very “pure” form it is also visible from a comparison of the free ions with  $\text{Hg}_2\text{Cl}_2$  and  $\text{Hg}_2(\text{CN})_2$ , Table 2.

We conclude for the case of Hg crown ether complexes that a very large coupling constant might be obtained for a preferably only weakly polarized system based on 18-crown-6 in which the positions trans to the respective other heavy metal are not accessible by coordinating solvent molecules due to steric bulk. This could perhaps be achieved by using a suitably substituted crown ether. However, the theoretical requirement of a symmetric system for a large coupling constant would also make it more difficult to detect. According to the computational data, a system similar to **1** but without the possibility of a solvent molecule coordinating Hg through the 18-crown-6 ring would also be a promising candidate for a large coupling constant in the range of 350 kHz. Again, introducing some steric bulk in

the crown ether could perhaps achieve this. Another candidate could be a system with only one crown ether for which a weakly nucleophilic solvent could reduce the polarization of the  $\text{Hg}_2^{2+}$  fragment through coordination to the free mercury.

**The  $[\text{Hg}–\text{Hg}–\text{Hg}]^{2+}$  System: One-Bond and Two-Bond Coupling, Solvent Effects, and Counterions.** The two-bond coupling constant  ${}^2J(\text{Hg}–\text{Hg})$  in  $\text{Hg}_3^{2+}$  has so far not been observed experimentally. From our calculations for the bare ion, Table 1, with 464.1 kHz the coupling constant turns out to be substantially larger than  ${}^1J(\text{Hg}–\text{Hg})$  (242.9 kHz) by a factor of about 1.9. Spin–orbit effects are more pronounced for  ${}^2J(\text{Hg}–\text{Hg})$  than for  ${}^1J(\text{Hg}–\text{Hg})$  and lead to a reduction of  ${}^2J(\text{Hg}–\text{Hg})$  to approximately 400 kHz and a ratio of 1.7. Nevertheless,  ${}^2J(\text{Hg}–\text{Hg})$  is still strongly dominated by the scalar relativistic FC term. To rationalize the relative magnitudes of  ${}^2J(\text{Hg}–\text{Hg})$  and  ${}^1J(\text{Hg}–\text{Hg})$ , we again apply eq 1 together with Hückel theory. The Hückel MOs for this system (basis functions  $s_A$ ,  $s_B$ ,  $s_C$  for the three mercuries) are

$$\varphi_1 = \frac{1}{2}s_A + \frac{1}{\sqrt{2}}s_B + \frac{1}{2}s_C \quad (3a)$$

$$\varphi_2 = \frac{1}{\sqrt{2}}s_A - \frac{1}{\sqrt{2}}s_C \quad (3b)$$

$$\varphi_3 = \frac{1}{2}s_A - \frac{1}{\sqrt{2}}s_B + \frac{1}{2}s_C \quad (3c)$$

with orbital energies  $\alpha + \sqrt{2}\beta$ ,  $\alpha$ , and  $\alpha - \sqrt{2}\beta$ , for  $\epsilon_1$ ,  $\epsilon_2$  and  $\epsilon_3$ , respectively.  $\varphi_1$  and  $\varphi_2$  are occupied. From this, and eq 1, one can directly equate the ratio  ${}^2J(\text{Hg}–\text{Hg})/{}^1J(\text{Hg}–\text{Hg})$  to 3/2, without the need of knowing the particular values for the Hückel parameters  $\alpha$  and  $\beta$  or the hyperfine integral for the Hg 6s orbital. Taking the very approximate character of this approach into consideration, this result is in fair agreement with the ratio obtained from the ZORA DFT computations. The electronic density due to the Hg 6s orbitals for the  $\text{Hg}_3^{2+}$  system is according to this model predominantly located at the terminal mercuries, with a pronounced three-center character of the Hg–Hg bonds. This rationalizes the large magnitude of  ${}^2J(\text{Hg}–\text{Hg})$ .

Regarding the accuracy of the computational results, when compared to experiment, once more the necessity of modeling environmental effects becomes obvious. The system  $\text{Hg}_3^{2+}$  has been experimentally studied in liquid  $\text{SO}_2$ . If we include a few of these solvent molecules into the computation of the spin–spin coupling constants,  ${}^1J(\text{Hg}–\text{Hg})$  decreases drastically by about 50%. The data obtained for the structures **5–12** of Figure 2 are listed in Table 4. The interaction between  $\text{Hg}_3^{2+}$  and the  $\text{SO}_2$  molecules is very weak; therefore it is not reasonable to expect that any of the optimized structures displayed in Figure 2 represent a dominant structure with high abundance in the solution at the experimental temperature of 203 K. They have rather to be considered as snapshots during the time evolution of the system. Nevertheless, they illustrate the influence of the solvent on the Hg–Hg coupling constants in this system. Consideration of the counterions ( $\text{AsF}_6$ ) has essentially the same, if somewhat stronger, effect, viz. a strong reduction of  ${}^1J(\text{Hg}–\text{Hg})$ . Here, both an optimized structure and a known crystal structure could be employed for the computations, with very similar results. Because of the more qualitative aspect of the computations on  $\text{Hg}_3^{2+}$  in this section, we are not able to comment on the fact that models only including  $\text{SO}_2$  seem to

**Table 4.**  $^{199}\text{Hg}$ – $^{199}\text{Hg}$  Spin–Spin Coupling Constants in  $\text{Hg}_3^{2+}$  Coordinated by  $\text{SO}_2$  (solvent) or the Counterion  $\text{AsF}_6^-$  (in kHz)<sup>a</sup>, Based on Optimized Structures

| structure                | $^1J(\text{Hg}–\text{Hg})^b$ | $^2J(\text{Hg}–\text{Hg})$ |
|--------------------------|------------------------------|----------------------------|
| <b>5</b> <sup>c</sup>    | 103.3                        | 190.8                      |
| <b>6</b> <sup>d</sup>    | 101.1                        | 191.1                      |
| <b>7</b> <sup>d</sup>    | 109.3                        | 201.4                      |
| <b>8</b> <sup>d</sup>    | 110.6                        | 193.4                      |
| <b>9</b> <sup>d</sup>    | 118.0                        | 242.6                      |
| <b>10</b> <sup>d</sup>   | 135.9                        | 183.0                      |
| <b>11</b> <sup>d</sup>   | 115.6                        | 243.3                      |
| <b>12</b> <sup>d,e</sup> | 142.3                        | 153.8                      |
| expt. <sup>f</sup>       | 139.7(3)                     | g                          |

<sup>a</sup> Scalar ZORA DFT values for computational data, including the FC, OP, and OD terms. <sup>b</sup> Mean value of both one-bond coupling constants. <sup>c</sup> Based on crystal structure, Reference 36. <sup>d</sup> Optimized structure. <sup>e</sup> Optimization constrained to  $C_{2v}$  symmetry. <sup>f</sup>  $\text{Hg}_3(\text{AsF}_6)_2$  in  $\text{SO}_2$ , 203 K. <sup>g</sup> Experimental value for  $^2J(\text{Hg}–\text{Hg})$  not available.

perform better in comparison with experiment than the ones including the counterion. The reason for the strong reduction of  $^1J(\text{Hg}–\text{Hg})$  in the presence of solvent molecules or the counterions has again to be attributed to the mixing of the Hg–Hg antibonding  $\sigma^*$  orbital  $\varphi_3$  of eq 3c into the ground state when these molecules form weak bonds in particular to the terminal Hg's of  $\text{Hg}_3^{2+}$ , and the concomitant reduction of the s character of the Hg–Hg bond. The same analysis as in ref 12 holds in this case. The essence of the situation can already be described at the crude level of Hückel theory.

The two-bond coupling constant in  $\text{Hg}_3^{2+}$  is also strongly reduced in the presence of solvent molecules or counterions. The ratio between  $^2J(\text{Hg}–\text{Hg})$  and  $^1J(\text{Hg}–\text{Hg})$  remains  $>1$  for all of the optimized structures and generally appears to stay close to the ratio for the free ion. Therefore we predict an experiment in which this quantity could be measured for a not strongly polarized system to yield a value for  $^2J(\text{Hg}–\text{Hg})$  that is considerably larger than  $^1J(\text{Hg}–\text{Hg})$ , with an upper limit for the free ion in the range of 400 kHz.

Generally, we have not been able to converge geometry optimizations in which the starting geometry involved close coordination of the central Hg by solvent molecules, except (to some extent) for two cases, **10** and **12**. The latter was forced into a  $C_{2h}$  symmetric structure. In other cases the solvent molecules initially coordinating the central atom started to migrate to one of the terminal atoms during the course of the optimization. A number of geometry optimizations with solvent molecules coordinating to the terminal mercuries were successful instead. As already mentioned, the optimized structures that have been obtained from various starting geometries are displayed in Figure 2, with the resulting coupling constants being listed in Table 4. To qualitatively study the effect of coordination of a varying number of solvent molecules to either the central or the terminal metal atoms, we have carried out additional computations based on unoptimized geometries. The Hg–Hg distances have been adjusted to a mean value obtained for the respective optimized structures in Figure 2, as well as the Hg–O distance and the Hg–O–S and O–S–O angles. The general

tendency of the results (not shown) is that  $^1J(\text{Hg}–\text{Hg})$  becomes strongly reduced as compared to the free ion upon coordination of the terminal mercuries, with  $^2J(\text{Hg}–\text{Hg})$  ranging between 2 and 3 times the one-bond coupling, depending on the number of coordinating solvent molecules. The most extreme case was obtained for octahedral coordination of the terminal mercuries (i.e., for 10 solvent molecules in total) with  $^1J(\text{Hg}–\text{Hg}) = 98$  kHz and  $^2J(\text{Hg}–\text{Hg}) = 309$  kHz. In case only the central atom is coordinated,  $^1J(\text{Hg}–\text{Hg})$  tends to be close to or even larger than the corresponding value for the free ion, whereas  $^2J(\text{Hg}–\text{Hg})$  is very strongly reduced (down to  $^2J(\text{Hg}–\text{Hg}) = 75$  kHz for a four-coordinated central atom, with 245 kHz for  $^1J(\text{Hg}–\text{Hg})$ ). Intermediate cases (both central and terminal atoms coordinated) lead to intermediate results, as expected. The structures **10** and **12** also belong to this category. On the basis of the experience during the geometry optimizations, and the results from the systematic study on the unoptimized systems, it can be expected that coordination of the terminal mercuries will dominate in solution, with some minor coordination of the central atom on average due to the dynamics of the system. This can further be expected to reduce  $^1J(\text{Hg}–\text{Hg})$  to range between 100 and 150 kHz (expt. 140) with  $^2J(\text{Hg}–\text{Hg})$  being roughly twice as large. Because most of our calculations on the optimized systems do not exhibit coordination of the central Hg, it is obvious why the calculated values on average tend to be somewhat too small in comparison to experiment.

#### 4. Summary

We have demonstrated in this work that even subtle effects on the Hg–Hg bond due to the environment of the metal–metal(–metal) fragments can result in drastic changes of  $^1J(\text{Hg}–\text{Hg})$  and  $^2J(\text{Hg}–\text{Hg})$ . For this reason the upper limit for Hg–Hg spin–spin coupling constants has not yet been reached by experiments. Two effects have to be considered when estimating the magnitude of  $^1J(\text{Hg}–\text{Hg})$ : *coordination*, i.e., the formation of more or less strong bond between the metal atoms and surrounding ligands, solvent molecules, or counterions, and *polarization* of the metal–metal fragment due to different coordinating ligands. Both effects tend to reduce  $^1J(\text{Hg}–\text{Hg})$  in  $\text{Hg}_2^{2+}$ . For  $\text{Hg}_3^{2+}$ , we have shown that surrounding solvent molecules decrease both  $^1J(\text{Hg}–\text{Hg})$  and  $^2J(\text{Hg}–\text{Hg})$  considerably, through a preferred coordination of the terminal mercuries. It can be expected that  $^2J(\text{Hg}–\text{Hg})$  is substantially larger than  $^1J(\text{Hg}–\text{Hg})$  for this system.

On the basis of the analysis it appears that systems with Hg–Hg bonds remain promising candidates for the measurement of extremely large nuclear spin–spin coupling constants. A weakly polarized, not axially coordinated system based on  $\text{Hg}_2^{2+}$  could potentially exhibit a value of 500 kHz or higher.

**Acknowledgment.** This work has received financial support from the National Science and Engineering Research Council of Canada (NSERC). Parts of the computations have been carried out at the computational facilities of the MACI cluster at the University of Calgary (www.maci.ca). One of us (T.Z.) acknowledges a Canada Research Chair from the Canadian Government.

(36) Cutforth, B. D.; Davies, C. G.; Dean, P. A. W.; Gillespie, R. J.; Ireland, P. R.; Ummat, P. K. *Inorg. Chem.* **1973**, *12*, 1343–1347.